Challenging Glass 6 - Conference on Architectural and Structural Applications of Glass
Louter, Bos, Belis, Veer, Nijsse (Eds.), Delft University of Technology, May 2018.

ISBN 978-94-6366-044-0, https://doi.org/10.7480/cgc.6.2119

The Effects of Cold Warping on Glass Stiffness

Austin Bensend
Enclos, USA, abensend@enclos.com

Significant progress has been made during the past two decades to advance the use of cold warped glazing (glass that has been elastically twisted out of plane) to achieve architectural vision. As with most new technologies, a full understanding of the mechanics of elastic cold warping has lagged its adoption and increasing specification for use in new construction. As a contractor whose aim is to turn vision into reality, Enclos has been invested in research and development related to the structural and performance implications of cold warped glazing. One of the most recent discoveries from this work at Enclos has been to relate cold warping of glass to its effect on plate stiffness. In particular, transverse stiffness to resist load may be negatively affected by the operation of cold warping glass supported by a perimeter frame. This loss in stiffness has been observed in cold warped glass when compared to flat glass of equal size and thickness. Recent work at Enclos indicates deflection due to transverse load increases with an increasing degree of warping. This phenomenon is especially pronounced for thin plates that resist load through significant large-deformation, non-linear plate behavior. As the degree of warp increases, the loss of stiffness becomes increasingly apparent, to the point at which the glass buckles. As a result of the warping operation, compressive membrane stresses are generated in the center region of the glass. These compressive stresses counteract the tension that normally arises during large-deformation plate behavior and that contributes to its deflection performance. As such, a membrane compression due to warping leads to the loss in stiffness when membrane effects appreciably contribute to overall bending stiffness (as they do in plates that fall within the large-deflection regime of bending). An exploration of this phenomena using a series of finite element tests, coupled with observations from previous testing are the basis for these findings.

Keywords: Cold Warped Glass, Deflection, Stiffness

1. Introduction

Within the last two decades, one of the more visible changes in the architectural glazing industry has been the increasing prevalence of freeform three-dimensional complex glazing projects. Many different strategies exist to achieve the architectural vision of three-dimensional singly- and doubly-curved glazed surfaces. Among these strategies are cold bending (Figure 1a), which is elastic bending of glass, and cold warping (Figure 1b), which is elastic twisting of glass.

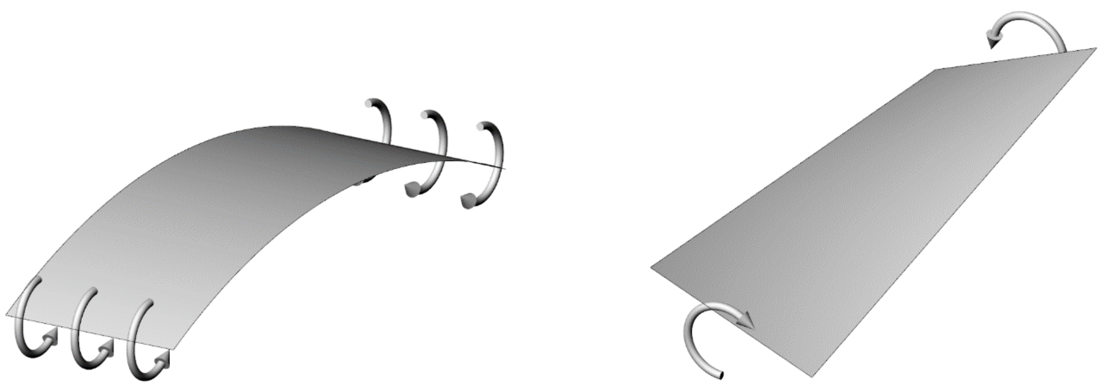

a) b)

Fig. 1a) Cold bending and b) Cold warping

Although it may seem counterintuitive, glass can exhibit significant flexibility prior to rupture. This is especially apparent in cold bending and cold warping of relatively thin glass that is heat treated or chemically tempered to improve its capacity for deformation. Cold bending and cold warping both impose form onto otherwise flat glass by forcing them via their supports into a deformed, albeit stressed shape. These approaches have been key to readily achieving complex surfaces in practice. Previous work at Enclos has been focused specifically on the realm of cold warping, and this body of work is no exception. However, the work contained herein is unique in that it contains an exploration on the effect that cold warping has on the stiffness of glass when subjected to a uniform lateral pressure.

The desire to harness the flexibility of glass to enforce a desired surface geometry has led to the recognition that decreasing the thickness of glass allows an increase in deformability and a decrease in required holding forces at the supporting structure to generate the deformed shape. In the category of cold warping, as previous work at Enclos (Bensend 2015; Bensend 2016) and by others (Staaks 2003; Eekhout et. al. 2004; Van Laar 2004; Hoogenboom 2004; Besserud et.al. 2012; Galuppi et.al. 2014) has shown, glass that is too thin has its own drawbacks – namely:

- Reduced capacity to resist transverse load
- Limited ability to be warped without buckling
- Increased deflection under transverse load

Thus, in the realm of cold warping there exists an optimal thickness for a given size, geometry, and required load resistance. Too thick and the glass is difficult to deform without breakage or without excessive holding forces. Too thin, and the glass may buckle, may not have sufficient capacity for transient load cases, or may exhibit excessive transverse deflection during anticipated loading.

While a framework has been established to quantify transverse load capacity and buckling resistance of warped glazing (Bensend 2015; Bensend 2016), less is known about the effects that cold warping has on deflection due to transverse load. Careful consideration of the in-service deflection behavior of warped glass is vital for sound engineering practice. It may be tempting to dismiss cold warping as having little effect, if any, on the glass stiffness. However, for cases where the glass derives a portion of its stiffness from membrane effects, any change to membrane stress arising from warping may reasonably be expected to alter the glass stiffness. The numerical studies presented herein confirm that membrane stresses due to cold warping can significantly decrease the stiffness of perimeter-supported glass relative to the same warped geometry without residual membrane stresses from warping.

2. Background

Where membrane stress effects are negligible or not present, a plate or shell is said to follow small deflection theory. In this case, the mid-depth of the material does not undergo any appreciable strain when loads are applied. For plates supported at their perimeters, a widely cited rule of thumb is that small deflection theory is valid for cases when deflections during transverse loading are less than one-half the plate thickness. This is analogous to a beam in bending, where lateral loads are resisted primarily in flexure of the beam. In this case, membrane stresses do not contribute significantly to the overall stiffness of the beam or plate.

However, when the mid-depth of the plate is strained during application of transverse load, the plate is said to follow large deflection theory. In this case, the deflected shape allows for transverse loads to be resisted by a combination of flexure and axial stresses. For rectangular flat plates, the tensions that develop near the center are resisted by a membrane compression ring near the perimeter, as seen in Figure 2. In this case, the plate deforms sufficiently so that it carries loads via axial and bending stresses, rather than by bending stress alone.

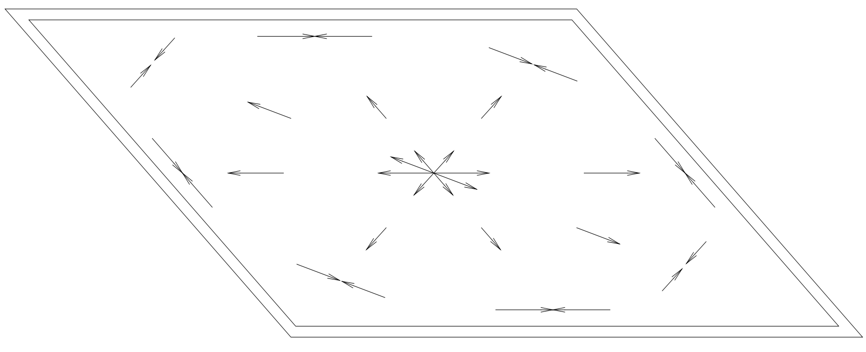

Fig. 2 Membrane tension resisted by membrane compression ring in thin plate

Where membrane effects contribute to the stiffness of plate materials, deflection is not linear with the application of load. The result is that deflections increase with load, but at a decreasing rate. Unlike small deflection theory, this is no longer analogous to a beam in bending. Rather, it is more like a cable, in that the deflected shape directly affects the stiffness. Taking the cable analogy one step further, when the prestress of a tensioned cable is reduced, its lateral deflection increases. In a similar way, if membrane compressions are present in the center region of a thin plate, the stiffness at a given level of load would be less, compared to a plate that is not in a state of membrane compression at its center.

It has been established that cold warping from flat to a hyperbolic paraboloid shape generates membrane compressions at region in the middle of the plate surface, surrounded by a membrane tension region near the perimeter of the plate. Previously recorded instances of buckling observed during cold warping and published numerical studies (Staaks 2003; Eekhout et. al. 2004; Van Laar 2004; Hoogenboom 2004; Besserud et.al. 2012; Galuppi et.al. 2014; Bensend 2015; Bensend 2016) support the understanding that membrane compressive stresses are present in cold warped glass which is otherwise unloaded. Based on the background provided in this section, this is precisely the condition that is expected to result in a loss of transverse stiffness in thin plates.

3. Finite Element Study of Twist Ratio Effect on Stiffness

To investigate the impact of warping on transverse stiffness, a set of finite element models were created and analyzed. These models are the same as had been analyzed in previous research at Enclos to quantify the buckling tendency of rectangular, cold warped plates (Bensend, 2016). The models ranged from aspect ratios of 1:1 to aspect ratios of 5:1, and short dimensions of rectangular glass from *B*=400mm to *B*=1500mm, as seen in Table 1.

Table 1: Finite element model specimens for each aspect ratio considered

Short Dimension, *B* [mm]	1st Thickness, *t* [mm]	2nd Thickness, *t* [mm]	3rd Thickness, *t* [mm]
400	2.16	2.92	--
480	2.16	2.92	--
600	2.16	2.92	3.78
800	2.92	3.78	4.57
1500	5.56	7.42	9.02

The test specimens chosen consisted of a set of five families of finite element models, where each family corresponded to a distinct aspect ratio of long to short dimension. Aspect ratio families modeled were 1:1, 1.2:1, 1.5:1, 2:1 and 5:1. The magnitude of twisting out of plane was defined using the dimensionless twist ratio, *k*. This ratio provided a convenient way to enforce warped geometry in consistent deformation steps, regardless of plate geometry and thickness. The ratio *k* is defined in Equation 1, and is believed to be roughly constant at the point of buckling (Bensend 2016).

$$k = \left(\frac{d}{t}\right) \cdot \left(\frac{B}{\sqrt{B^2 + L^2}}\right) \tag{1}$$

d = corner displacement arc length out of plane [mm]

t = glass thickness [mm]

B = short dimension [mm]

L = long dimension [mm]

Figure 3 conveys graphically many of the variables required to determine twist ratio, *k*. Figure 3 also provides a representation of the support scheme that has been used to enforce the warped shape. At the supports, drawn as small pyramids, the glass is free to rotate and to translate locally in plane; supports only resist translation out of plane, normal locally to the surface. Two of the corner nodes of the finite element model were fixed in additional translation degrees of freedom as required to provide stability from global translation and rotation. The finite element models were developed using a cylindrical coordinate system for ease of enforcing the warped geometry while not providing any stiffness in the plane of the plate. Out of plane deflections, *h*, were measured locally normal to the surface at the mid-span intersection of the panel length and width.

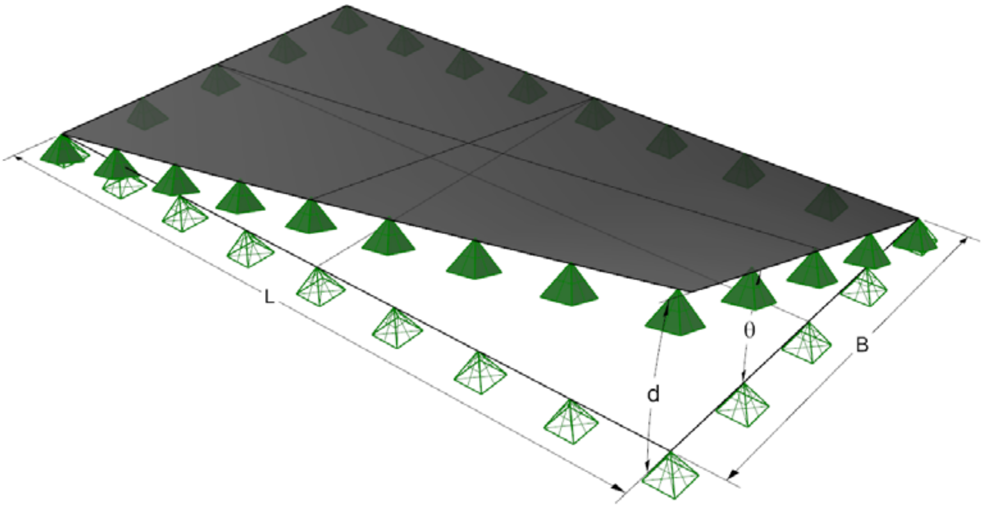

Fig. 3 Warping geometry nomenclature and support locations

Each model was incrementally deformed, starting from an un-warped shape where twist ratio k=0 to a warped shape beyond the point of buckling, where k=16.2. Twist ratios modeled are provided in Table 2. Buckling occurred in the finite element models within +/-5% of the deformation step where k=13.5, designated $k_{buckling}$. Post-buckling deformation is significantly more than pre-buckled deformation. Therefore, only results from deformation increments 1 through 9 have been considered in this paper. In practice, warping would likely be capped at an even lower twist ratio than this to safely avoid buckling.

Table 2: Deformation increments

Deformation Increment	Twist Ratio, k	Percentage of $k_{buckling}$ [%]
1	0	0%
2	0.675	5%
3	1.35	10%
4	2.7	20%
5	5.4	40%
6	8.1	60%
7	10.8	80%
8	11.475	85%
9	12.15	90%
10	12.825	95%
11	13.5	100%
12	14.175	105%
13	14.85	110%
14	15.525	115%
15	16.2	120%

At the initial un-deformed shape and after each subsequent twist increment, lateral pressures were applied and removed in a series of 15 load steps, ranging from 0.0 kPa to 2.0 kPa back to 0.0 kPa. As a result, each finite element model contained a series of 225 load/deformation steps. At each step, the lateral deformation at the midspan of the surface was recorded and plotted against the twist ratio, k, for a given lateral pressure.

For simplicity purposes, the results here have been abridged to summarize only the 1.0 kPa lateral load magnitude. Midspan deflections of the surface relative to the unloaded position are provided and plotted in Figures 4 to 8. It is apparent that an increased twist ratio, k, results in a decreased transverse stiffness for all specimens analyzed. Some of the specimens exhibited significant loss of stiffness, resulting in deflections that were two or more times the magnitude as observed in the un-warped condition. Numerical result values have been provided in Appendix A.

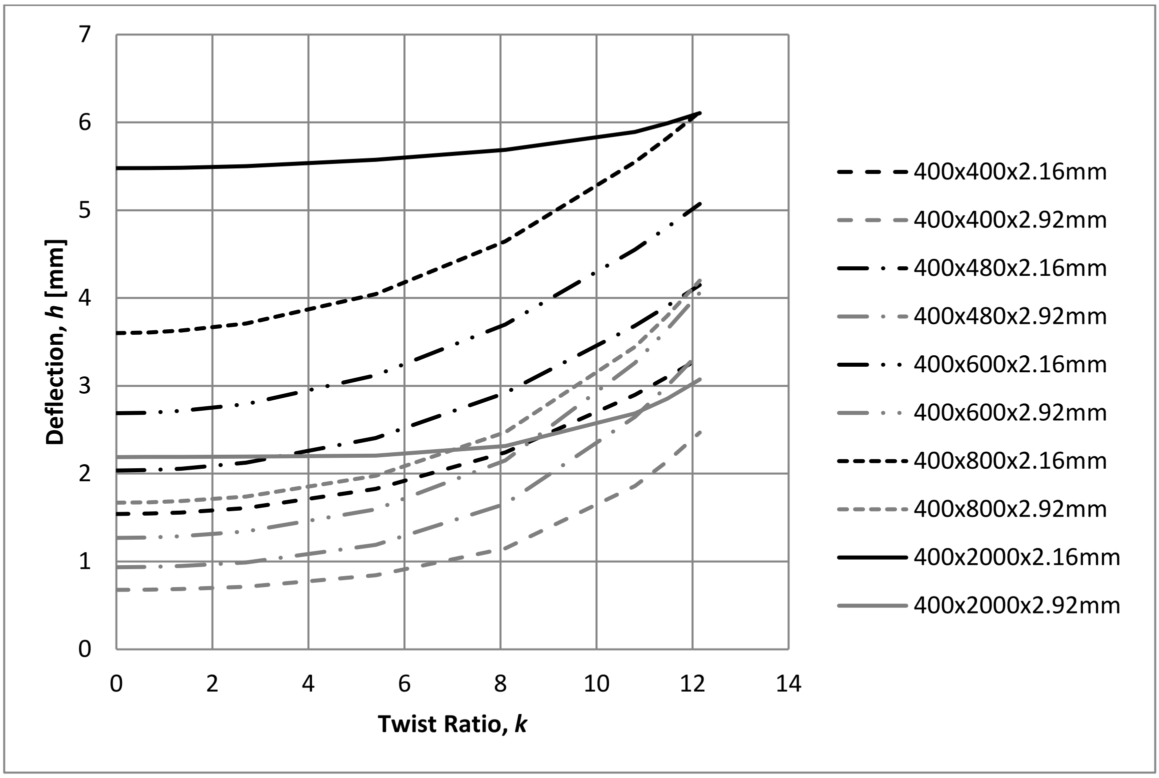

Fig. 4 Transverse deflection of 400mm wide specimens at 1.0 kPa

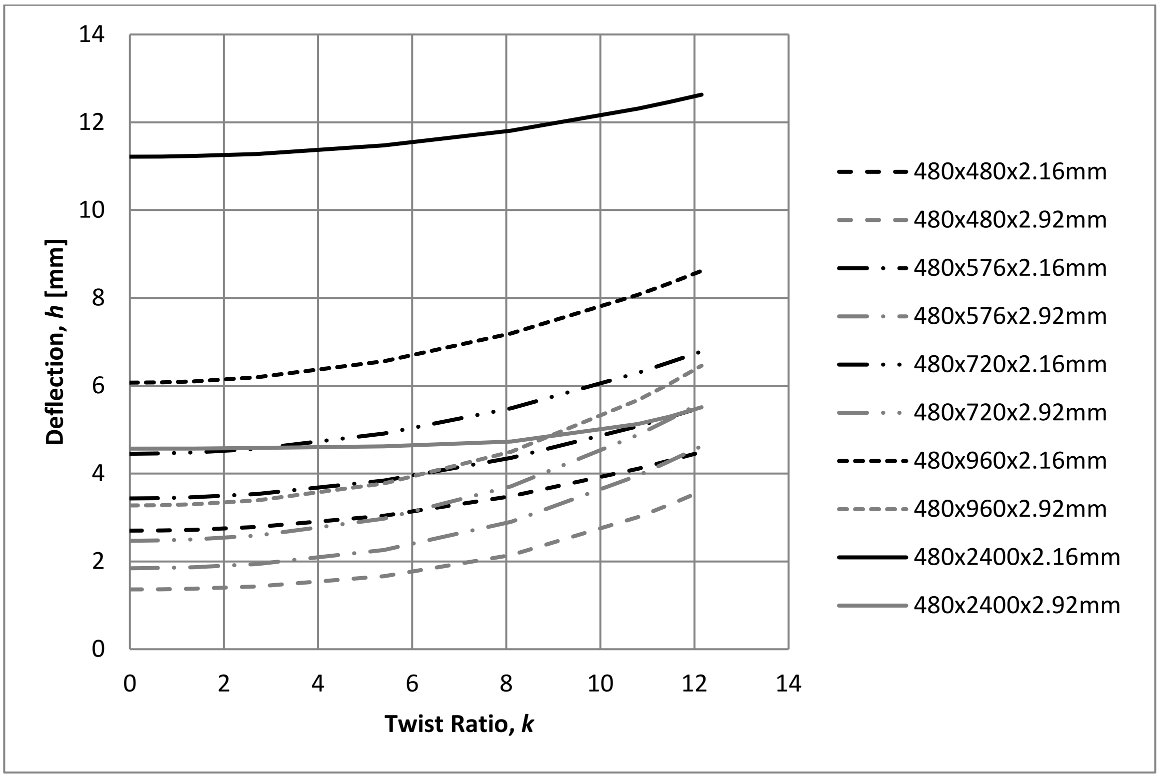

Fig. 5 Transverse deflection of 480mm wide specimens at 1.0 kPa

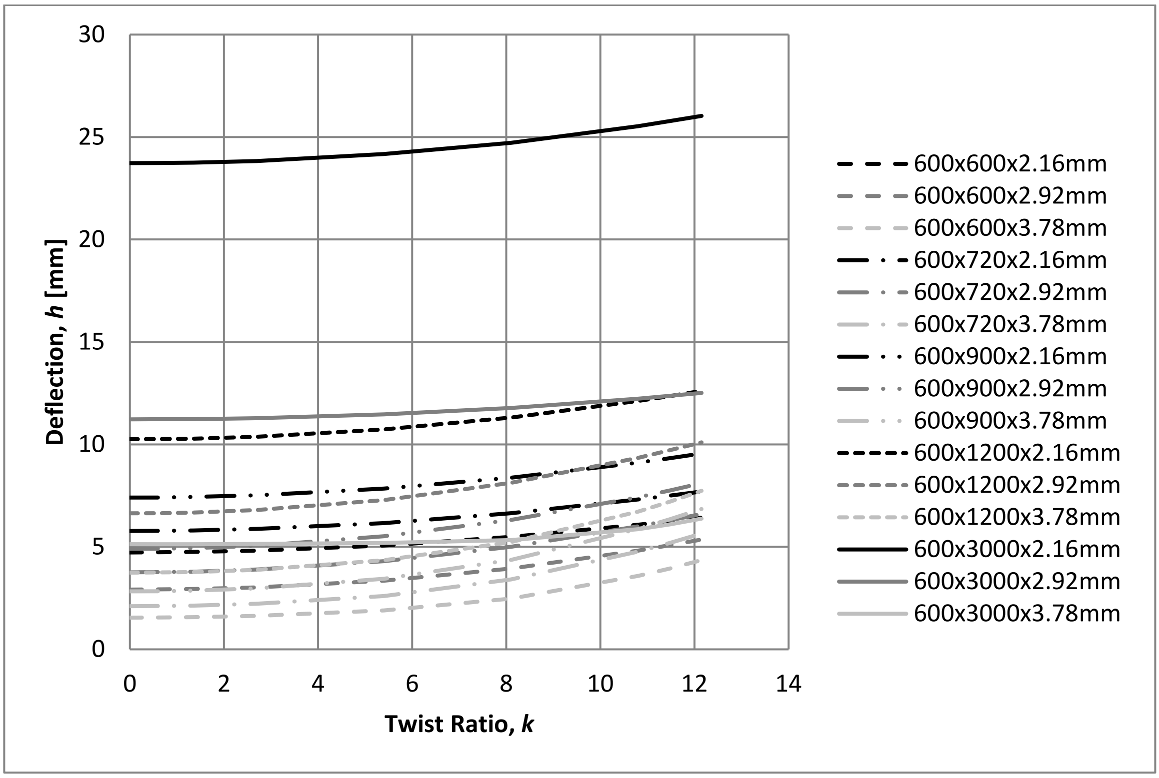

Fig. 6 Transverse deflection of 600mm wide specimens at 1.0 kPa

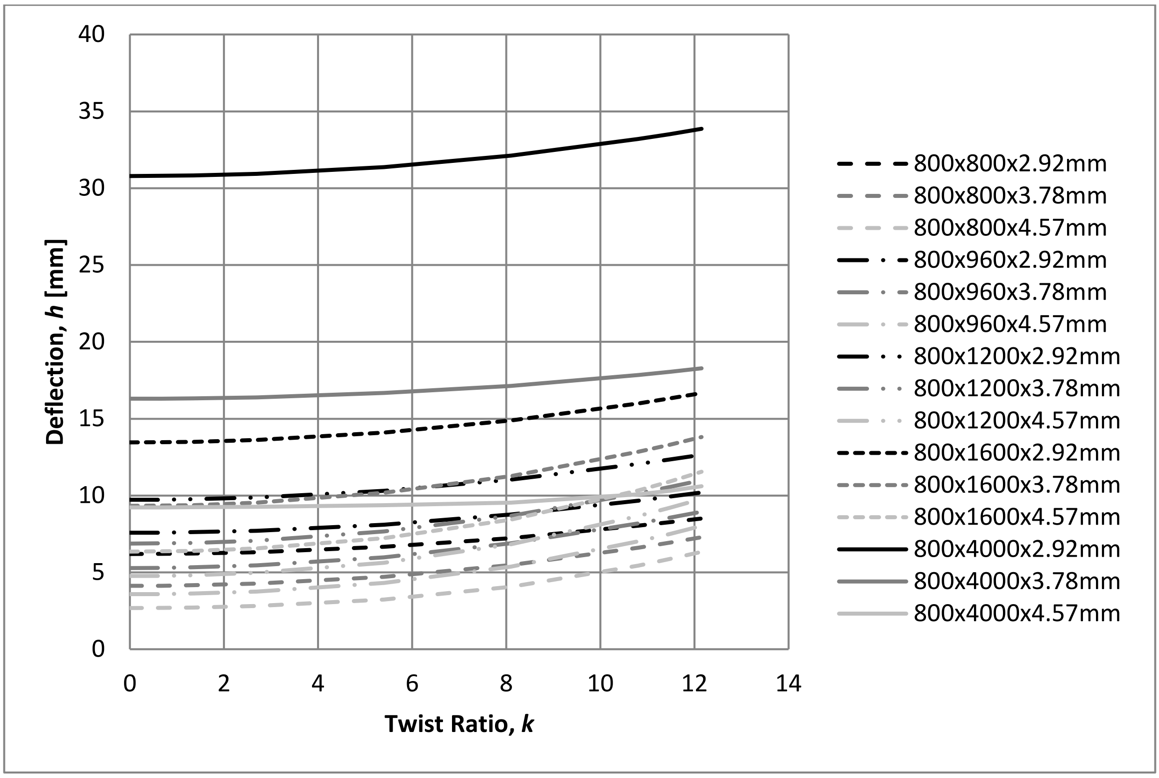

Fig. 7 Transverse deflection of 800mm wide specimens at 1.0 kPa

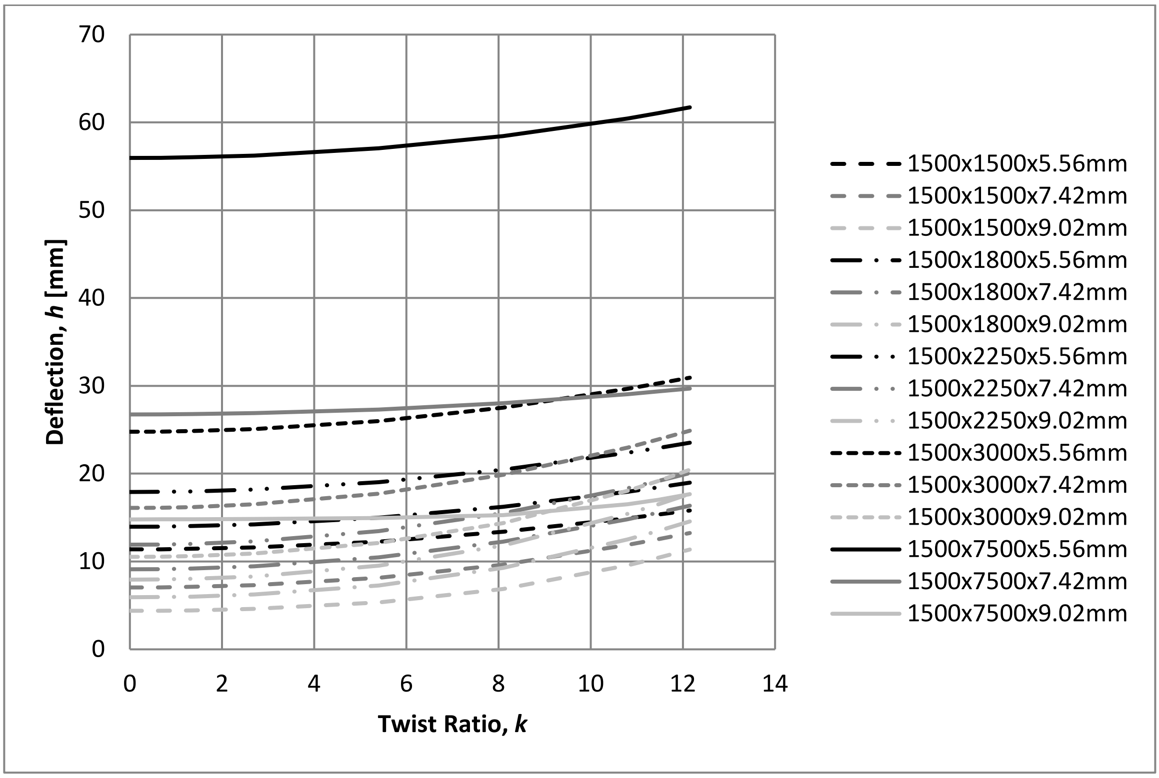

Fig. 8 Transverse deflection of 1500mm wide specimens at 1.0 kPa

During testing conducted at Enclos in the spring of 2015, observations during testing confirm this loss of stiffness (Bensend 2015). As the threshold for buckling was approached and crossed, the transverse glass stiffness was observed, albeit in an anecdotal way based solely on physical interactions with the warped specimens. When the specimen reached the point of anticipated buckling, the glass was able to be readily and visibly deformed at its center using a small force. As seen in Figure 9, a specimen approximately B=1524mm tall x L=2286mm wide x t=9.02mm thick piece of glass had been deformed approximately d=228mm out of plane and could be deformed easily with a force small enough to be imposed from a pinky finger. Based on the specimen and warpage dimensions, the glass had barely entered the buckled realm, with twist ratio k=14.0.

Fig. 9 Deformation of 9.02mm thick glass using the pinky finger method

4. Finite Element Study of Residual Stress Effects

A separate finite element study was then conducted to investigate the effect of the residual stress while maintaining the same surface geometry. Two specimens were investigated, both with t=5.56mm, with short dimension B=1500mm and long dimensions of L=1500mm and L=3000mm, respectively. Both specimens were warped to the same twist ratio, k=8.1. Thus, the 1500mm x 1500mm specimen was warped out of plane to corner displacement d=63.67mm, while the 1500mm x 3000mm specimen was warped out of plane to d=100.64mm.

For each of the specimens, two residual stress cases were analyzed. The first case was a model that included the residual stresses from warping. Transverse load was then applied to this model in series of load increments up to 2.0 kPa. The second case was a model generated with the warped shape of the first case, this time without any residual stresses. The second model included the same transverse load steps as the first. Thus, this second model shared warped geometry with the first one; however, no residual warping stresses were included. The comparison of these two cases demonstrates the effect that warping stresses have on transverse stiffness when all else is equal.

The residual membrane stresses present in the cold warped 1500mm x 1500mm specimen are shown in Figure 10. In Figure 10, the maximum and minimum principal stresses at mid plane are shown, where black is the lowest and white is the highest principal stress. Direction 11 is the maximum principal residual stress and direction 22 is the minimum principal residual stress; a negative number indicates compression. What is seen in this figure is that a compression well exists at the center of the glass, while a tension ring exists around the perimeter. This creates a residual stress state that is opposite of that shown in Figure 2 for a thin plate resisting transverse pressure. As a result, the residual stresses present from warping counteract those that are generated during large deformation plate behavior. By extension, the residual warping stresses generated are counterproductive to providing stiffness for a thin plate subjected to transverse load.

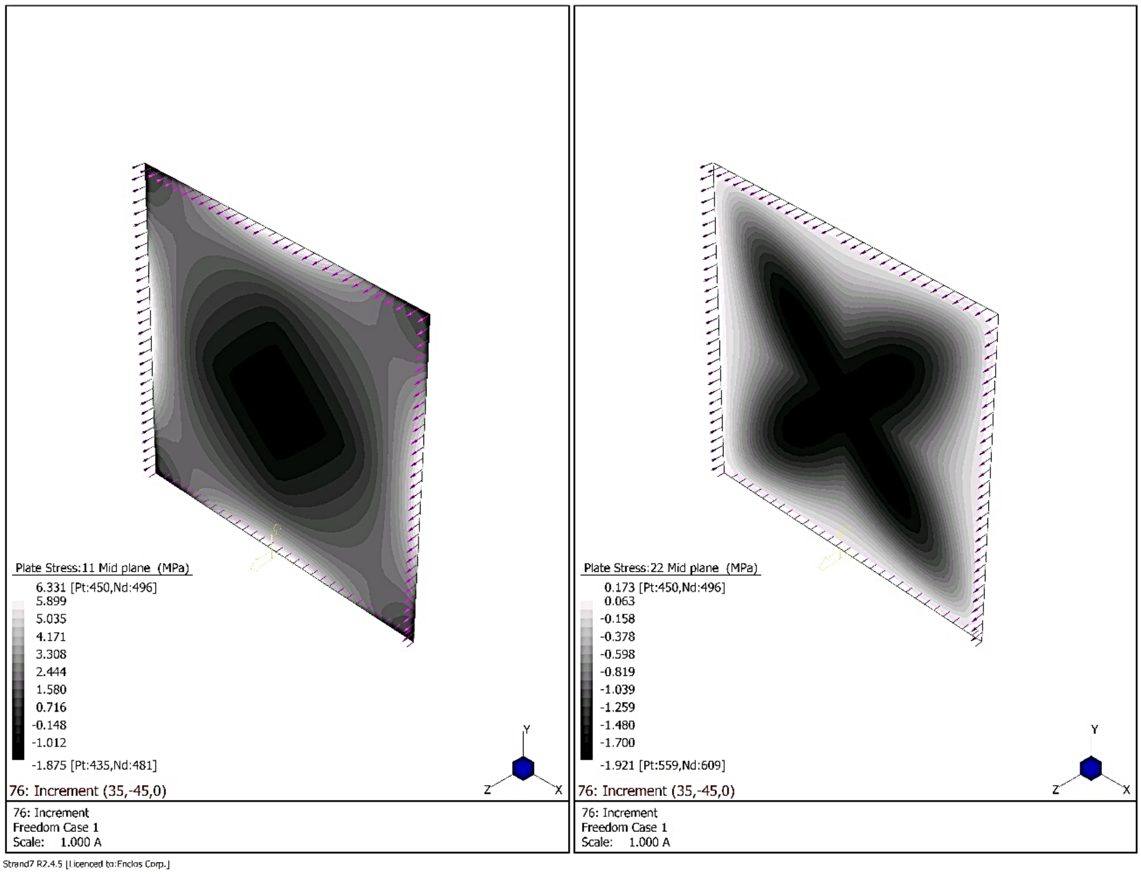

Fig. 10 Membrane stresses present in the 1500mm x 1500mm case including residual warping stress

To confirm the loss of stiffness arises from residual warping stresses, a comparison plot of mid-span deflection, h, versus lateral pressure has been provided in Figure 11 for both residual stress states of both specimens. This chart shows that for both specimens, the presence of warping residual stresses coincides with a loss in transverse stiffness. Numerical result values have been provided for reference in Appendix B.

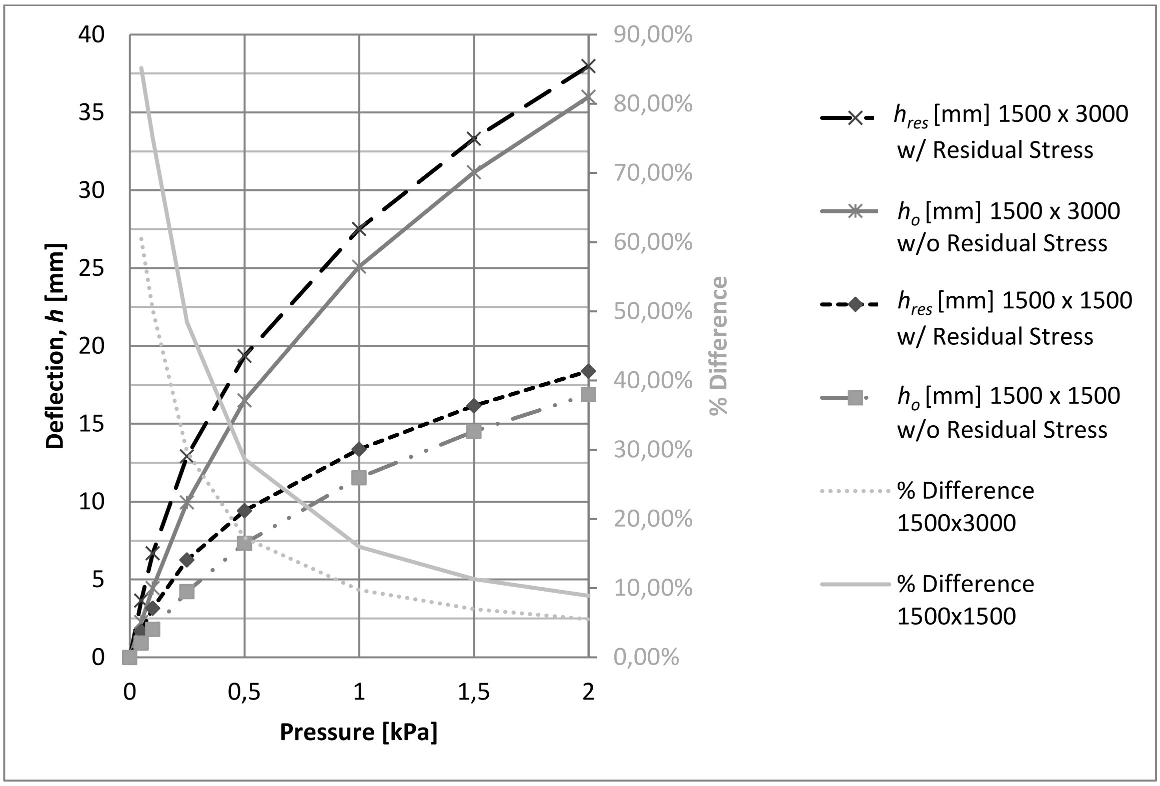

Fig. 11 Comparison of transverse deflection with and without inclusion of warping residual stresses

This loss is at its highest percentage for the lower transverse pressures, but is still pronounced even at the higher levels of lateral pressure. The light gray lines, plotted against the secondary axis in Figure 11 provide the percent difference between the cases with and without residual stress. The percent difference between deflection with and without residual warping stresses was calculated from Equation 2, where:

$$\%\,DIfference = \frac{h_{res} - h_o}{h_o} \times 100\% \quad (2)$$

h_{res} = mid-span deflection out of plane, including residual warping stresses [mm]

h_o = mid-span deflection out of plane, not including residual warping stresses [mm]

As postulated, from these finite element studies it appears that the presence of residual membrane stresses induced during the warping is a cause for the loss in stiffness of cold warped glass. It is reasonable to anticipate this result may be replicated across a variety of glass dimensions, thicknesses, transverse pressures, and twist ratios.

5. Conclusion

In conclusion, residual stresses from cold warping have been shown to reduce the transverse stiffness of cold warped glass. The effects that residual warping stresses have on the overall glass stiffness can be significant. As such, the impact that cold warping has on glass stiffness should not be ignored in the design and engineering of systems that specify deflection performance. This is especially apparent for cases where a significant portion of the overall glass stiffness is derived from membrane effects. Furthermore, at relatively small levels of transverse pressure, the effects warping stress has on transverse stiffness may be even more pronounced on a percentage basis.

While cold warped glass continues to be specified, investigated, and incorporated into new construction, fascinating new insights such as this relationship between cold warping stress and transverse stiffness are being uncovered. Informed design based on these findings is vital to successfully and reliably meeting or exceeding performance objectives. As insights like this one are revealed and subsequently considered, the proper use and incorporation of cold warped glazing into well performing systems may continue to occur with increasing degrees of confidence and success.

References

Bensend, A.: Beneath the surface: buckling of cold formed glass. In: Glass Performance Days 2015 Conference Proceedings, pp. 241-246, Glass Performance Days, Tampere, 24-26 June 2015

Bensend, A.: Maximizing the twist of cold formed glazing. In: Challenging Glass 5 Conference on Architectural and Structural Applications of Glass. Belis, Bos, & Louter (eds.), pp. 65-80, Ghent University, Belgium (2016)

Besserud, K., Bergers, M., Black, A.J., Carbary, L.D., Misson, D., and Rubis, K.: Durability of cold-bent insulating-glass units. Journal of ASTM International (JAI), 9(3), 205-242 (2012). doi:10.1520/JAI104120

Eekhout, M., Staaks, D., and Van Herwijnen, F.: Cold bent glass sheets in façade structures. Structural Engineering International (SEI), 14(2), 98-101 (2004)

Galuppi, L., Massimiani, S., Royer-Carfagni, G.: Buckling phenomena in double curved cold-bent glass. Int. J. Nonlin. Mech. 64, 70-84 (2014). doi: 10.1016/j.ijnonlinmec.2014.03.015

Hoogenboom, P.C.J.: SEI discussion on paper: Cold bent glass sheets in façade structures. Structural Engineering International (SEI), 14(4), 322 (2004)

Staaks, D.: Koud torderen van glaspanelen in blobs. Thesis, TU Eindhoven, Netherlands (2003)

Van Laar, H.: Stabiliteit van in het werk vervormde glaspanelen voor dubbelgekromde gevels. Thesis, TU Delft, Netherlands (2004)

Appendix A: Numerical Results Data at 1.0kPa

For further information, a summary of the results for the 1.0kPa transverse pressure across a range of specimens and twist ratios, *k*, is provided in Table A1 below.

Table A1: Deflections at 1.0kPa transverse pressure

Specimen	$k = 0$	$k = 0.675$	$k = 1.35$	$k = 2.7$	$k = 5.4$	$k = 8.1$	$k = 10.8$	$k = 11.475$	$k = 12.15$
400x400x2.16mm	1.54	1.55	1.56	1.61	1.83	2.24	2.90	3.10	3.31
400x400x2.92mm	0.68	0.68	0.69	0.71	0.85	1.15	1.86	2.14	2.47
400x480x2.16mm	2.04	2.04	2.06	2.12	2.41	2.92	3.68	3.91	4.15
400x480x2.92mm	0.94	0.94	0.95	0.99	1.19	1.66	2.65	3.00	3.38
400x600x2.16mm	2.69	2.70	2.72	2.79	3.12	3.70	4.55	4.81	5.07
400x600x2.92mm	1.27	1.27	1.29	1.34	1.59	2.15	3.26	3.64	4.06
400x800x2.16mm	3.60	3.61	3.63	3.71	4.04	4.64	5.55	5.82	6.12
400x800x2.92mm	1.67	1.67	1.69	1.74	1.98	2.47	3.44	3.80	4.20
400x2000x2.16mm	5.48	5.48	5.49	5.50	5.57	5.69	5.89	5.99	6.11
400x2000x2.92mm	2.19	2.19	2.19	2.19	2.21	2.32	2.69	2.86	3.07
480x480x2.16mm	2.70	2.71	2.72	2.78	3.04	3.48	4.11	4.30	4.49
480x480x2.92mm	1.36	1.37	1.38	1.43	1.66	2.14	3.01	3.29	3.60
480x576x2.16mm	3.43	3.44	3.46	3.54	3.84	4.36	5.08	5.29	5.51
480x576x2.92mm	1.84	1.85	1.87	1.94	2.26	2.90	3.96	4.28	4.63
480x720x2.16mm	4.45	4.46	4.48	4.57	4.91	5.49	6.30	6.53	6.78
480x720x2.92mm	2.47	2.48	2.50	2.59	2.97	3.71	4.88	5.24	5.62
480x960x2.16mm	6.07	6.08	6.10	6.19	6.56	7.19	8.08	8.34	8.62
480x960x2.92mm	3.27	3.28	3.30	3.39	3.77	4.50	5.67	6.05	6.46
480x2400x2.16mm	11.22	11.22	11.23	11.28	11.48	11.81	12.31	12.46	12.63
480x2400x2.92mm	4.57	4.57	4.57	4.58	4.62	4.73	5.13	5.30	5.51
600x600x2.16mm	4.73	4.73	4.75	4.81	5.07	5.49	6.08	6.25	6.43
600x600x2.92mm	2.92	2.92	2.94	3.02	3.36	3.95	4.82	5.08	5.36
600x600x3.78mm	1.55	1.55	1.57	1.63	1.90	2.48	3.58	3.95	4.35
600x720x2.16mm	5.78	5.78	5.80	5.87	6.17	6.65	7.31	7.50	7.70
600x720x2.92mm	3.76	3.77	3.79	3.89	4.30	5.00	6.00	6.29	6.60
600x720x3.78mm	2.11	2.11	2.13	2.22	2.61	3.41	4.77	5.20	5.65
600x900x2.16mm	7.41	7.41	7.43	7.52	7.84	8.38	9.12	9.33	9.56
600x900x2.92mm	4.91	4.92	4.94	5.06	5.52	6.31	7.43	7.76	8.11
600x900x3.78mm	2.83	2.84	2.86	2.97	3.44	4.36	5.88	6.35	6.85
600x1200x2.16mm	10.26	10.26	10.29	10.37	10.73	11.31	12.12	12.36	12.61
600x1200x2.92mm	6.64	6.65	6.68	6.80	7.29	8.13	9.35	9.71	10.10
600x1200x3.78mm	3.74	3.75	3.78	3.88	4.34	5.23	6.72	7.21	7.74

Table A1: (continued): Deflections at 1.0kPa transverse pressure

Specimen	$k = 0$	$k = 0.675$	$k = 1.35$	$k = 2.7$	$k = 5.4$	$k = 8.1$	$k = 10.8$	$k = 11.475$	$k = 12.15$
600x3000x2.16mm	23.73	23.73	23.75	23.84	24.16	24.73	25.53	25.77	26.03
600x3000x2.92mm	11.22	11.23	11.24	11.28	11.47	11.78	12.23	12.37	12.51
600x3000x3.78mm	5.13	5.13	5.14	5.15	5.19	5.33	5.87	6.10	6.38
800x800x2.92mm	6.20	6.20	6.22	6.31	6.66	7.23	8.03	8.26	8.50
800x800x3.78mm	4.13	4.14	4.16	4.27	4.71	5.48	6.61	6.94	7.29
800x800x4.57mm	2.68	2.69	2.71	2.81	3.22	4.05	5.44	5.87	6.34
800x960x2.92mm	7.58	7.59	7.61	7.71	8.11	8.77	9.67	9.93	10.20
800x960x3.78mm	5.28	5.29	5.32	5.45	5.98	6.89	8.18	8.55	8.95
800x960x4.57mm	3.58	3.60	3.63	3.76	4.31	5.37	7.01	7.50	8.02
800x1200x2.92mm	9.72	9.73	9.76	9.87	10.31	11.05	12.05	12.34	12.65
800x1200x3.78mm	6.87	6.89	6.92	7.07	7.67	8.69	10.13	10.55	11.00
800x1200x4.57mm	4.77	4.78	4.82	4.97	5.63	6.83	8.65	9.20	9.78
800x1600x2.92mm	13.46	13.47	13.50	13.62	14.10	14.89	16.00	16.32	16.66
800x1600x3.78mm	9.33	9.34	9.38	9.54	10.18	11.27	12.84	13.31	13.81
800x1600x4.57mm	6.35	6.36	6.40	6.56	7.22	8.44	10.33	10.92	11.55
800x4000x2.92mm	30.79	30.80	30.82	30.93	31.37	32.12	33.19	33.52	33.86
800x4000x3.78mm	16.30	16.31	16.32	16.39	16.67	17.14	17.84	18.05	18.28
800x4000x4.57mm	9.23	9.23	9.24	9.26	9.36	9.53	10.07	10.31	10.61
1500x1500x5.56mm	11.39	11.40	11.44	11.61	12.27	13.38	14.90	15.34	15.81
1500x1500x7.42mm	7.05	7.06	7.11	7.31	8.15	9.65	11.88	12.54	13.25
1500x1500x9.02mm	4.39	4.40	4.44	4.61	5.34	6.86	9.55	10.42	11.37
1500x1800x5.56mm	13.96	13.98	14.03	14.22	14.98	16.23	17.95	18.45	18.98
1500x1800x7.42mm	9.12	9.14	9.20	9.45	10.47	12.26	14.82	15.57	16.36
1500x1800x9.02mm	5.93	5.95	6.01	6.24	7.25	9.26	12.51	13.51	14.56
1500x2250x5.56mm	17.92	17.93	17.99	18.20	19.05	20.45	22.38	22.94	23.53
1500x2250x7.42mm	11.92	11.94	12.01	12.30	13.47	15.48	18.34	19.18	20.07
1500x2250x9.02mm	7.94	7.96	8.03	8.31	9.52	11.82	15.43	16.53	17.70
1500x3000x5.56mm	24.78	24.80	24.86	25.08	26.00	27.53	29.65	30.27	30.93
1500x3000x7.42mm	16.11	16.13	16.20	16.51	17.74	19.88	22.98	23.91	24.90
1500x3000x9.02mm	10.53	10.55	10.62	10.90	12.11	14.38	18.03	19.19	20.45
1500x7500x5.56mm	55.96	55.97	56.02	56.22	57.04	58.44	60.46	61.06	61.71
1500x7500x7.42mm	26.75	26.75	26.78	26.88	27.31	28.04	29.07	29.37	29.69
1500x7500x9.02mm	14.79	14.79	14.80	14.84	14.97	15.30	16.51	17.03	17.67

Appendix B: Numerical Results Data for Residual Stress Comparison Study

For further information, a summary of the results for two specimens is provided in Table B1 and Table B2 below. These specimens are *B*=1500mm x *L*=1500mm x *t*=5.56mm and *B*=1500mm x *L*=3000mm x *t*=5.56mm, each with two residual stress cases: with residual warping stresses and without residual warping stresses. The analysis covers a range of transverse pressures. Both specimens consider the case where twist ratio, k = 8.1.

Table B1: Transverse deflection of 1500mm x 1500mm x 5.56mm specimen at *k*=8.1

Load [kPa]	h_{res} [mm]	h_o [mm]	% Difference
0.00	0.00	0.00	-
0.05	1.69	0.91	85.16%
0.10	3.15	1.80	75.00%
0.25	6.26	4.22	48.42%
0.50	9.43	7.33	28.65%
1.00	13.38	11.54	15.96%
1.50	16.15	14.51	11.32%
2.00	18.39	16.89	8.89%

Table B2: Transverse deflection of 1500mm x 3000mm x 5.56mm specimen at *k*=8.1

Load [kPa]	h_{res} [mm]	h_o [mm]	% Difference
0.00	0.00	0.00	-
0.05	3.65	2.28	60.47%
0.10	6.68	4.45	50.18%
0.25	12.92	9.96	29.72%
0.50	19.37	16.51	17.29%
1.00	27.53	25.09	9.72%
1.50	33.32	31.15	6.95%
2.00	37.98	36.00	5.50%